Enhanced Convection and Rainfall over Mesoscale Gradients of Antecedent Soil Moisture Anomalies in Subtropical South America

Divyansh Chug[1], Francina Dominguez[1], Christopher Taylor[2], Cornelia Klein[2,3], Steve Nesbitt[1]

[1]University of Illinois Urbana Champaign, [2]UK Center for Ecology and Hydrology, [3]University of Innsbruck

I. Why are we doing this research?

Mesoscale heterogeneity on the surface can affect the location and diurnal timiing of convection, and change the strength and sign of SM-PPT feedbacks

1. La Plata basin (black bounday in Fig. 1) is one of the most important socio-economic regions in the world.

2. It supports 50% of the population and 70% of the GDP of Argentina, Bolivia, Brazil, Paraguay and Uruguay.

3. Convective storms in this region broadly account for >60% of the total warm season rainfall accumulation.

4. Life and economy are greatly affected by the skill in predicting the location and timing of convective storms.

5. Heterogeneous land cover, patchy rainfall and strong land-atmosphere interactions imply strong control of soil moisture (SM) on convection and precipitation (PPT).

Analysis domain is shown in Fig. 2 where the shading is topographic complexity, i.e. local standard deviation of elevation in a 40 km by 40 km region.

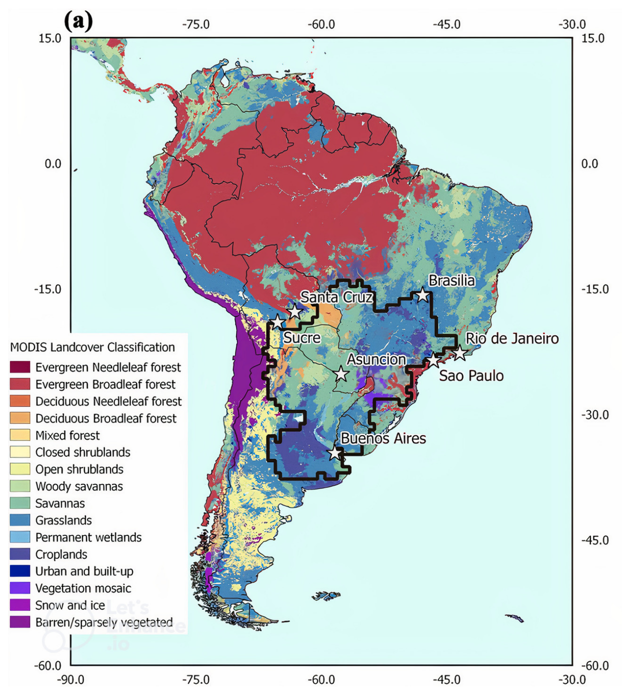

Fig. **1**. Land cover over South America

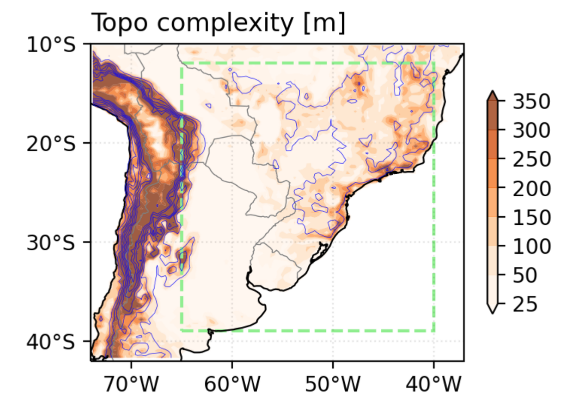

Fig. **2**. Topography over the domain

II. How are we doing this research?

We use the technique of *Taylor et al. (2011)* to find the fingerprint of SM heterogeneity in convective initiation (CI) events using satellite data

Variable	Source	Resolution
1. Brightness temperature	NCEP/ NOAA	4 km, 30 min
2. Land surface temperature	MODIS, AMSR2	5.6 km, daily 10 km, daily
3. Soil Moisture	SMAP	9 km, daily
4. Winds, CIN, CAPE	ERA5	0.25°, hourly
5. Elevation	GMTED	1 km, static
6. Vegetation index	MODIS	0.05°, monthly
7. Precipitation	IMERG	0.1°, 30 min

CI detection

We track the time/location of CI occurence for every 20 km x 20 km region in the domain, using infrared brightness temperature as follows:

1. Cold core temperature < 235 K

2. Maximum cloud size < 400 km^2

3. Isolated; no cloud pixels in vicinity

4. Rapidly cooling new cloud

Morning SM antecedent to daytime CI

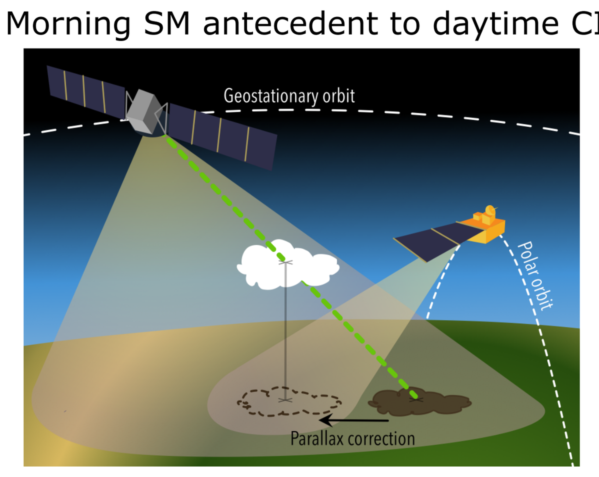

Fig. **3**. Schematic of data retrieval

We found **77,745 CI events** over the domain with an afternoon peak. Frequency of CI reduces toward higher latitudes.

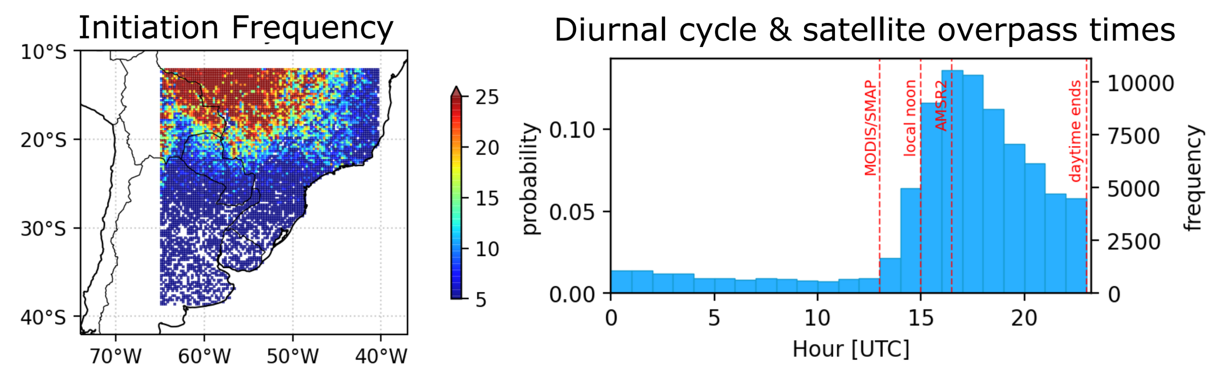

Fig. **4**. Frequency and diurnal cycle of detected CI events

Land surface anomaly patterns

1. Subtract seasonal cycle to get anomalies

2. Extract spatial transect underlying CI events

3. Align spatial transect along low-level wind

4. Subtract spatial mean from each transect

5a. Compute composite mean spatial pattern

5b. Calculate mean downwind gradient from CI location to a point 30 km downwind of CI

5c. Sample gradients from vicinity for significance testing

III. What did we find? Convection initiates preferentially over spatially drier/warmer patches at the mesoscale but the background wind controls the sign of SM-PPT feedbacks

1. Composite along-wind cross-sections of LST and SM anomalies show preferential CI over the downwind end of the spatially warmer/drier patch at tens of kilometers scale

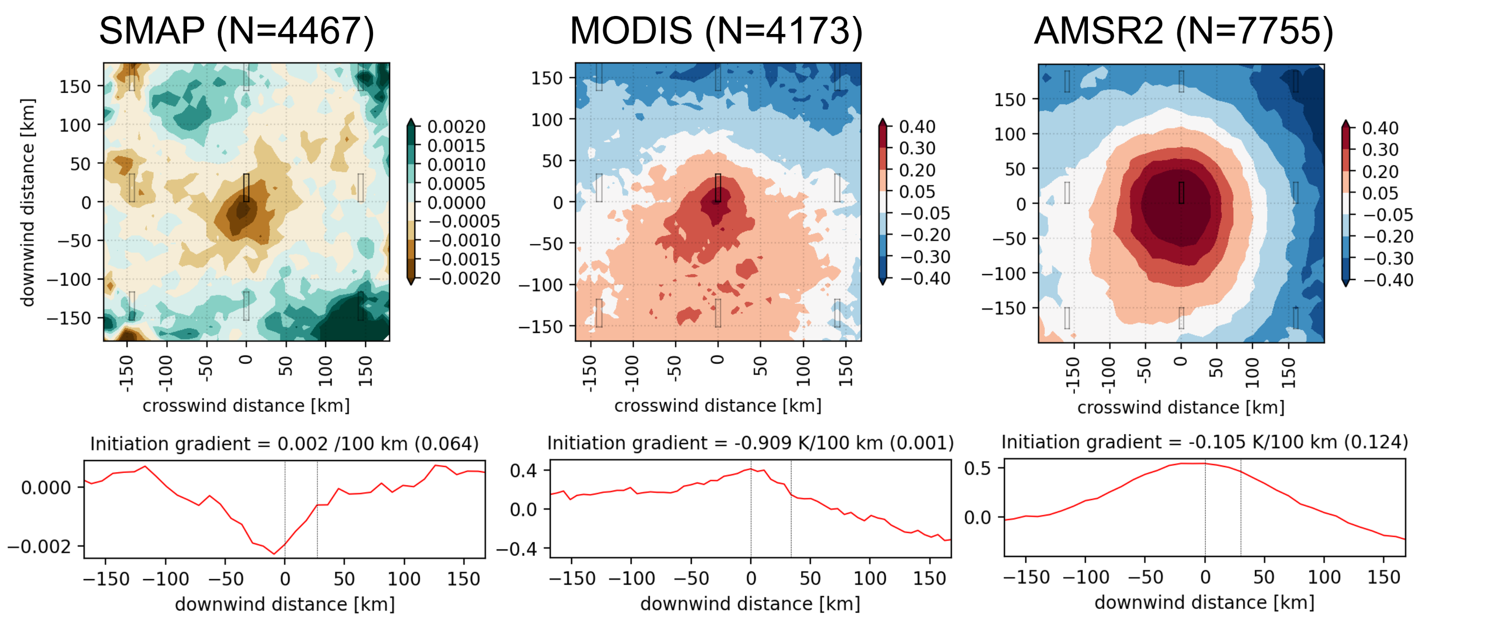

Fig. **5**. Composite mean anomalies of SM (cm^3/cm^3) and LST (K) underlying daytime CI cases (top) and one-dimensional transects through the center (bottom) showing the downwind initiation gradient along with its statistical significance in parenthesis

2. Composite spatial anomalies of MODIS LST computed from reclassified CI events based on environmental conditions show that CI occurs over strong negative gradients at 30-km scale during weak 10-m wind, low vegetation density, high CAPE and low CIN

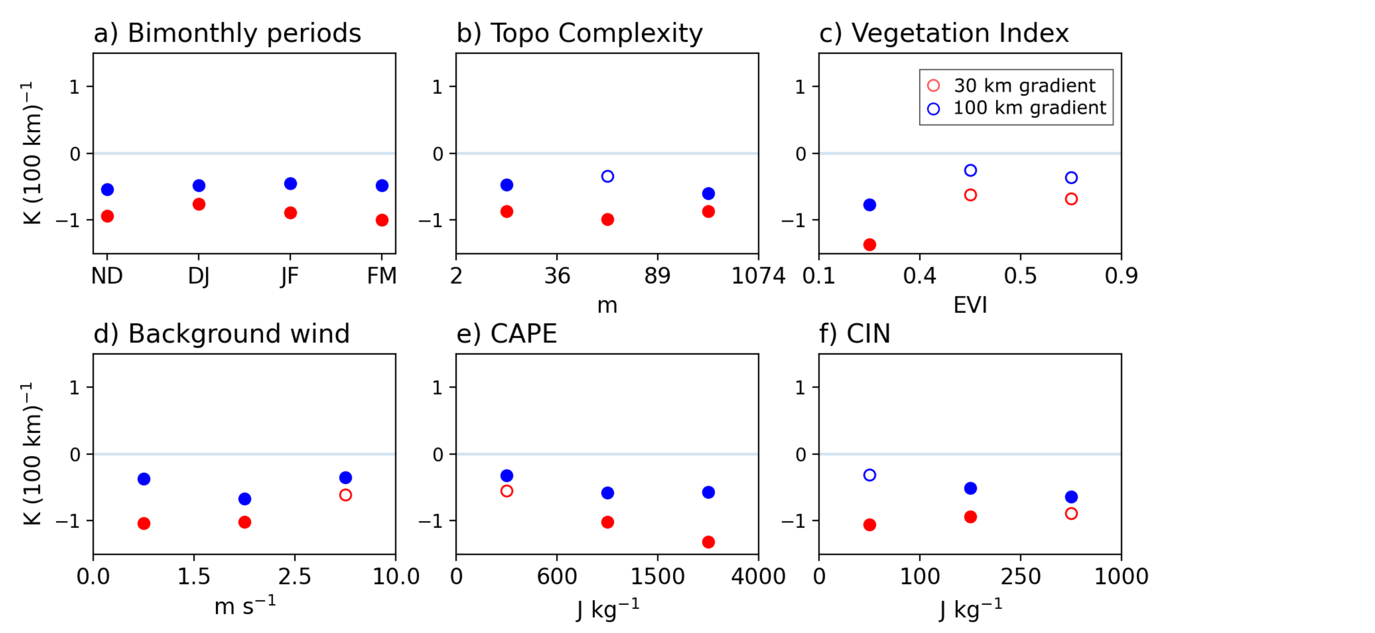

Fig. **6**. Mean downwind initiation gradients at 30 km and 100 km spatial scales from CI classes based on seasonality, topographic complexity, low-level wind, CAPE, CIN and EVI

3. All terciles of topographic complexity show strong negative LST gradients underlying CI location. However, the along-wind composites of elevation show that convection initiates against downslope background flow for cases in the highest TC tercile.

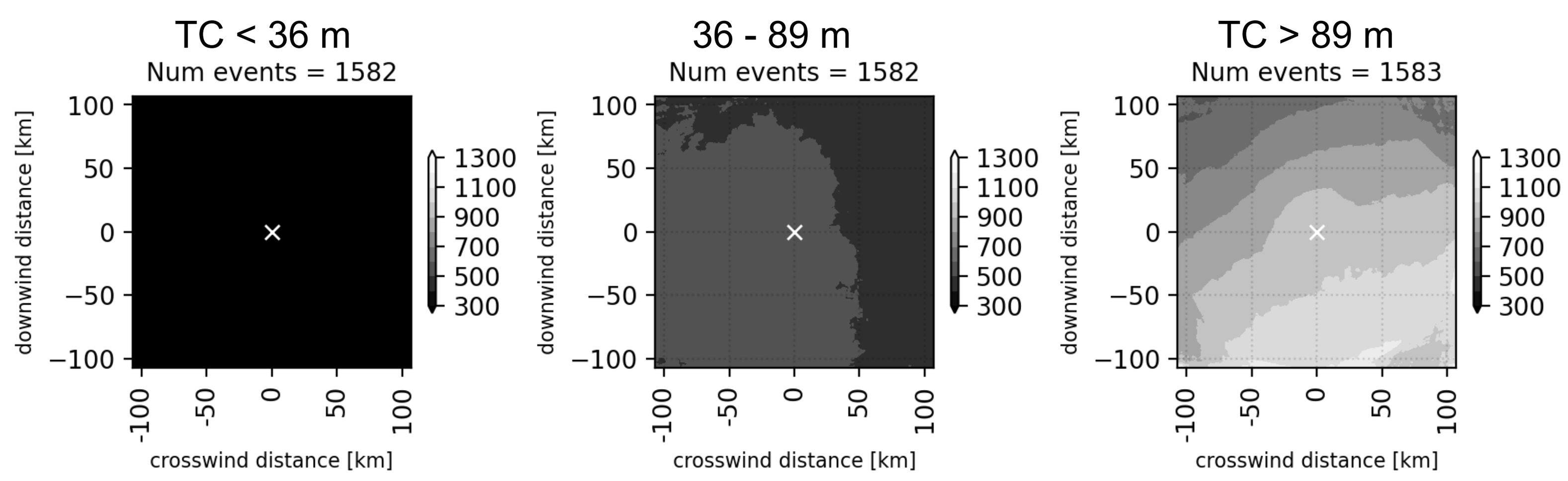

Fig. **6**. Mean along-wind elevation for CI classes based on threshold of topographic complexity - local standard deviation of elevation in a 40 km by 40 km region

We suspect the role of elevated heating and associated mountain-valley circulations in strengthening the SM heterogeneity-induced upslope wind through in-phase superposition.

Imamovic et al. (2017) showed that this interaction can enhance both CI and PPT for low (<125 m) topographic elevations.

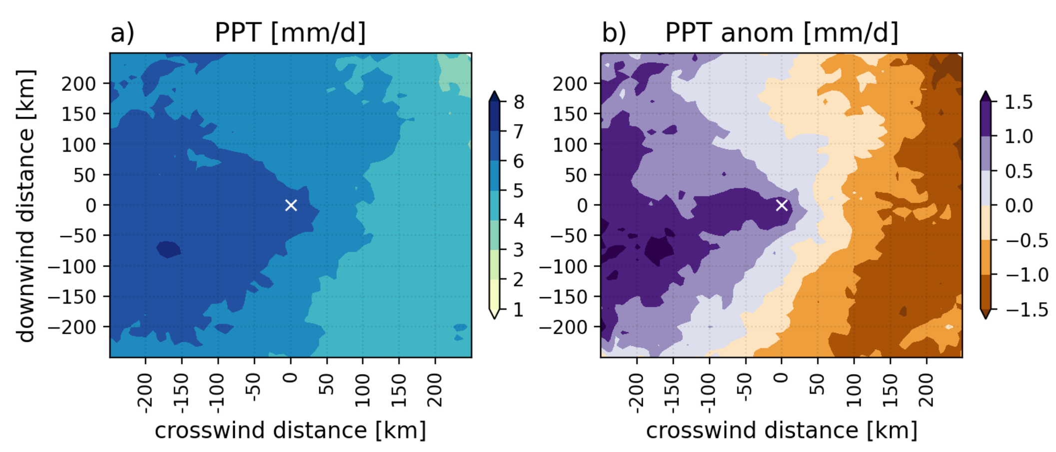

Fig. **7**. Composite along-wind rainfall accumulation over 24- and 48-hours following CI onset for the 4173 MODIS cases

4. The along-wind composite pattern of PPT and PPT anomaly in the 24 hours following the CI onset shows greater accumulation on the left side of the wind direction. As storms initiate against the northerly wind (bottom to top), the combination of storm propagation and translation leads to greater PPT on the eastward side of CI location.

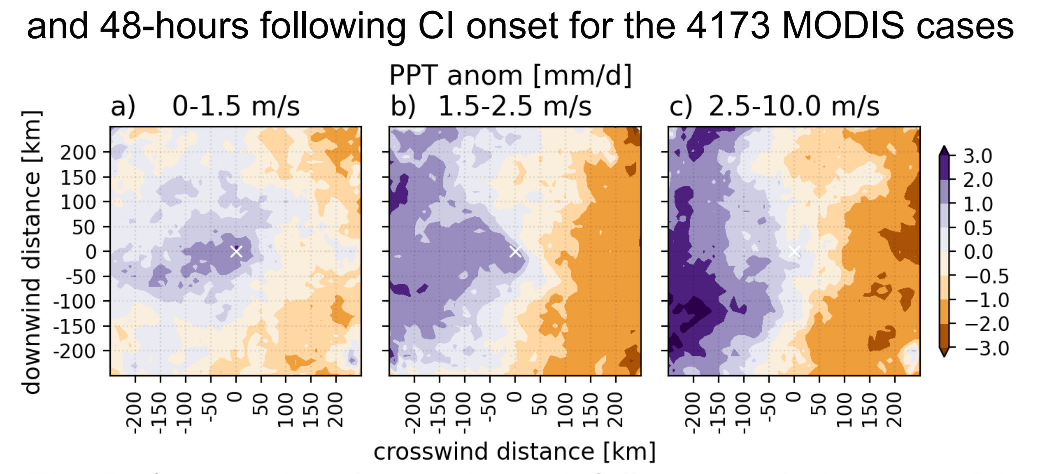

Fig. **8**. Composite along-wind rainfall accumulation over 24-hours following onset for CI cases classified by terciles of mean low-level wind speed in the two hours prior to initiation

5. Under low background wind conditions, the location of PPT maxima stays over the drier patch where convection initiated. This would lead to **negative SM-PPT feedback**. However, under strong background wind, the PPT maxima is located hundreds of kilometers upwind. **This can change the sign of the SM-PPT feedback**.

This effect of background wind and mid-tropospheric flow on the sign of SM-PPT feedbacks for CI over drier soil has been shown in numerical simulations by *Froidevaux et al, (2014)*. Under low background wind speeds, the wind profile cannot support the propagation of convective structures that dissipate after raining close to their updrafts, leading to a negative SM-PPT feedback.

IV. Conclusion - What mechanisms are at play?

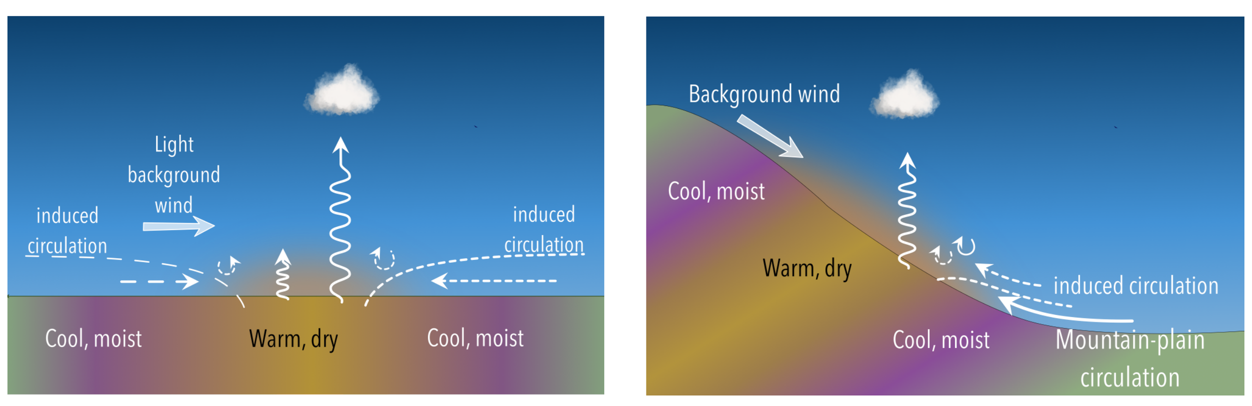

Fig. **9**. (Left) Idealized SM-induced flows (dashed arrows) under light synoptic wind shows preferred CI location at downwind end of dry patch. (Right) Superposition of induced flow with mountain-valley circulations.

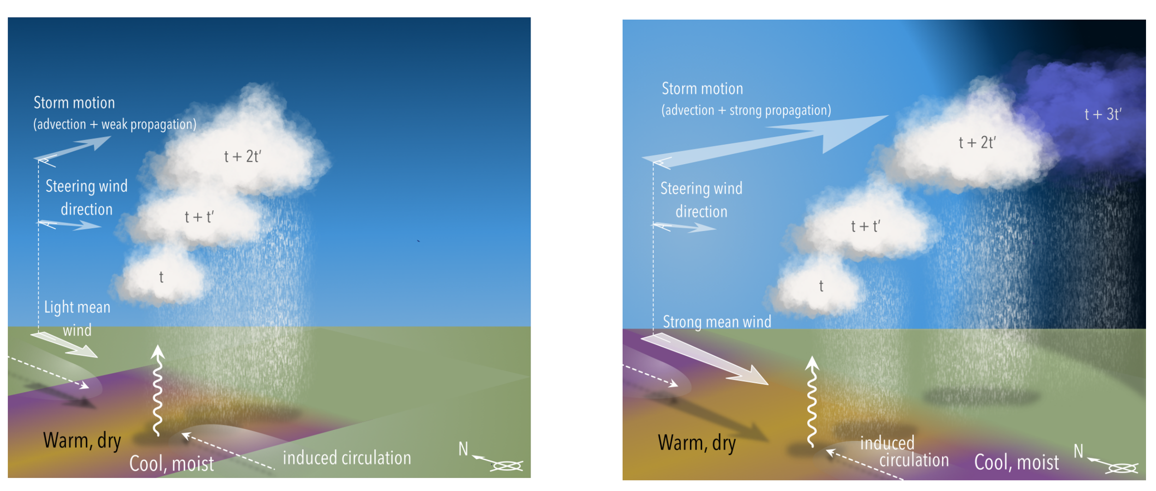

Fig. **10**. (Left) Location of maximum precipitation following convection over dry patches under light mean wind leads to negative SM-PPT feedbacks. (Right) Strong wind supports farther propagation of convective structures.

1. Convection in subtropical South America initiates preferentially over strong positive downwind gradients of SM and strong negative downwind gradients of land surface temperature, on the order of tens of kilometers.

2. Strong gradients at tens of kilometers are more likely to initiate convection during low background wind (<2.5 m/s), low CIN (< 250 J/kg), high CAPE (>1500 J/kg) and over low background EVI (<0.4).

3. Gradients of larger length scale are important for CI during conditions of moderate background wind and high CIN.

4. Over topographically complex regions, the SM-induced flows can interact with mountain-valley circulations due to elevated heating over the dry patch.

5. Rainfall accumulates preferentially on the upwind side following the CI.

6. With weak background wind prior to CI, the wind profile is too weak to support the propagation of convection features. Rainfall accumulates at and near the dry patch likely leading to a negative SM-PPT feedback.

7. Under strong low-level wind prior to CI, the location of precipitation maxima can translate hundreds of kilometers upwind from the dry patch. This can lead to a traditionally positive SM-PPT feedback.

V. Acknowledgements

The support for this research is acknowledged to the Future Investigators in NASA Earth and Space Science and Technology grant 80NSSC19K1352 awarded to DC, and National Science Foundation grant 1454089 awarded to FD.

We thank Susana Roque-Malo and Convey Science LLC for helping us summarize the research through graphical illustrations.

We also thank Sean Matus for reprojecting high resolution MODIS lake dataset to filter CI cases near water bodies.

VI. References

Taylor, C. M., Gounou, A., Guichard, F., Harris, P. P., Ellis, R. J., Couvreux, F., and De Kauwe, M. (2011): Frequency of Sahelian storm initiation enhanced over mesoscale soil-moisture patterns. *Nature Geoscience*, **4**, 430-433.

Imamovic, A., Schlemmer, L., and Schär, C. (2017): Collective impacts of orography and soil moisture on the soil moisture-precipitation feedback. *Geophysical Research Letters*, **44**(22), 11683-11691.

Froidevaux, P., Schlemmer, L., Schmidli, J., Langhans, W., and Schär, C. (2014): Influence of the background wind on the local soil moisture-precipitation feedback. *Journal of the Atmospheric Sciences*, **71** (2), 782-799.

Divyansh Chug
dchug2@illinois.edu
University of Illinois Urbana Champaign